

## STABILITY OF SYNCHRONIZATION IN A SHIFT-INVARIANT RING OF MUTUALLY COUPLED OSCILLATORS

R. YAMAPI

Department of Physics, Faculty of Science  
University of DOUALA, PO. Box 24157 DOUALA, Cameroon

R.S. MACKAY

Mathematics Institute  
University of Warwick, Coventry CV4 7AL, U.K.

(Communicated by the associate editor )

ABSTRACT. This paper treats synchronization dynamics in a shift-invariant ring of  $N$  mutually coupled self-sustained electrical units. Via some qualitative theory for the *Lyapunov* exponents, we derive the regimes of coupling parameters for which synchronized oscillation is stable or unstable in the ring.

### 1. Introduction.

Synchronisation of dynamical systems is a phenomenon of widespread technological and natural importance, ranging from the operation of electricity distribution networks to the neural generation of breathing rhythm, for example. It is of interest to determine the parameter regimes in which stable synchronisation can occur. There are many works on this, e.g. [1]- [15] and it would fill a book to review the literature.

Here we restrict attention to the simplest context for synchronisation, a shift-invariant ring of identical nearest neighbour coupled second order oscillators, and the strongest notion of synchronisation, identical time dependence. Such a system has been used to model a parallel operating system of microwave oscillators [16, 17], and the interest in synchronisation is to produce high power. This allows us to derive strong general results on the parameter regime for stable synchronisation. The key new ingredient is qualitative analysis of the parameter dependence of the time-dependent flow on projective space of an associated two-dimensional linearised system about a synchronous solution. The paper is developed around a specific electrical example, but the theory applies more generally.

The paper is organised as follows. In Section 2 the electrical system is described. In Section 3, basic results on linear stability of synchronous solutions of such a system are explained. In Section 4, the Prüfer transformation is used to develop extensive qualitative theory for a generalised class of linear equations; parts are deferred to appendices. In Section 5, the theory is compared to the results of numerics on the electrical system, with good agreement. Section 6 summarises the conclusions, gives a simple extension of the results, and suggests some directions for further work.

---

2000 *Mathematics Subject Classification.* Primary: 58F15, 58F17; Secondary: 53C35.

*Key words and phrases.* Synchronization, Master stability function, Lyapunov exponents.

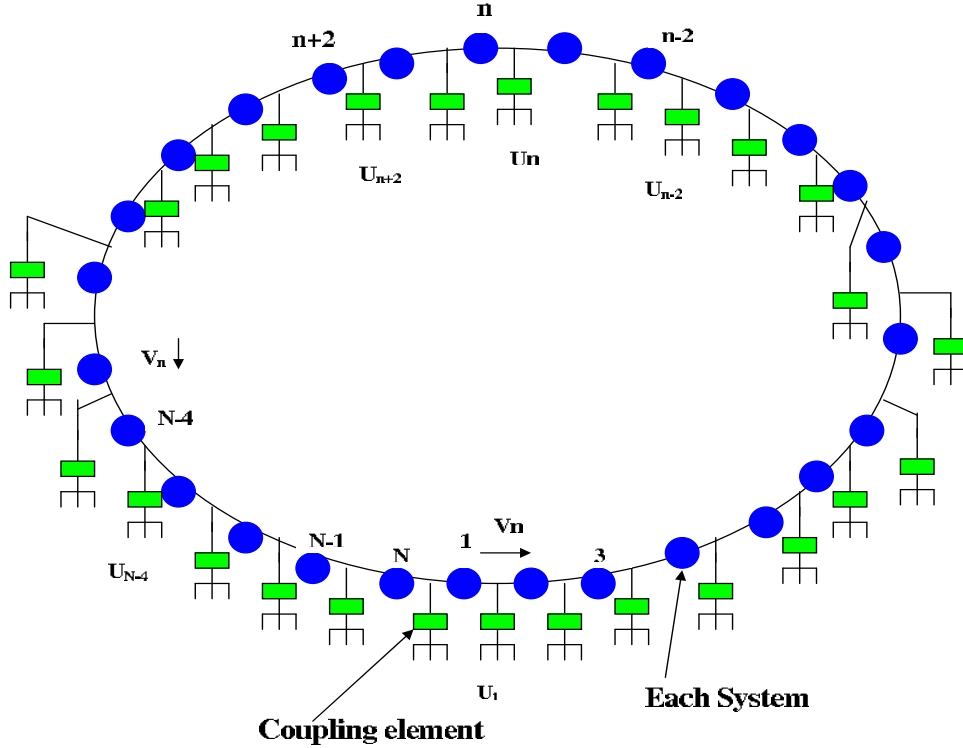


FIGURE 1. Schema of the ring of  $N$  mutually coupled self-sustained electrical units. The units are shown in Figure 2(a). The coupling elements are capacitors  $C_m$  to ground.

## 2. The electrical model.

We study a ring of  $N$  electrical units, as in Figure 1, where each unit consists of an inductor  $L$ , nonlinear resistor  $R$  and nonlinear capacitor  $C$  in series, as in Figure 2(a), and the coupling is via capacitors  $C_m$  to ground between each neighbouring pair of units.

The voltage  $V_C$  across each nonlinear capacitor is taken to depend on its charge  $q$  by

$$V_C = \frac{1}{C_0}q + a_3q^3, \quad (1)$$

where  $C_0$  is the linearised capacitance and  $a_3$  is a nonlinear coefficient depending on the type of capacitor in use. This is typical of nonlinear reactance components such as varactor diodes widely used in many areas of electrical engineering to design for instance parametric amplifiers, up-converters, mixers, low-power microwave oscillators, etc [18]. We allow the coefficient  $a_3$  to be of either sign, but if negative we should add some additional term for  $|q|$  large to keep  $V_C$  of the same sign as  $q$ . To simplify presentation we leave it out.

The current  $i$  through any capacitor is related to the charge  $q$  on it by

$$i = \frac{dq}{d\tau} \quad (2)$$

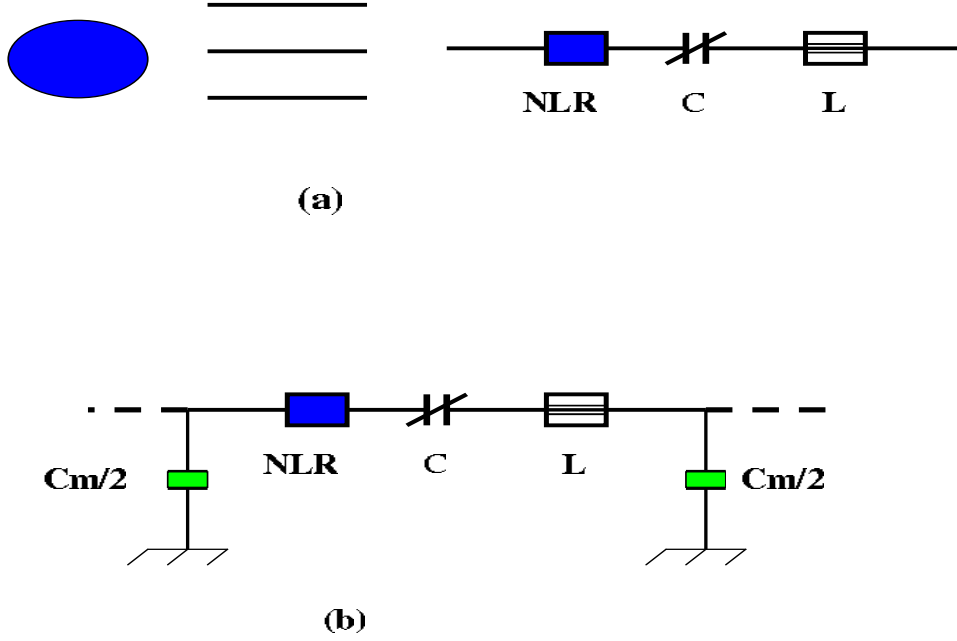


FIGURE 2. (a) Schema of each electrical unit; (b) Alternative schema of a unit including half the capacitors to ground at each end, which makes the unit self-exciting.

where  $\tau$  is time.

The voltage  $V_R$  across each nonlinear resistor is taken to depend on the current  $i$  through it by

$$V_R = R_0 i_0 \left[ -\left(\frac{i}{i_0}\right) + \left(\frac{i}{i_0}\right)^3 \right], \quad (3)$$

where  $R_0$  is its linearised negative resistance and  $i_0$  is the current at which the voltage changes to the same sign as  $i$ . This represents the effect of an amplifying device, e.g. transistor, and nonlinear saturation.

The voltage  $V_L$  across an inductor depends on the current  $i$  through it by

$$V_L = -L \frac{di}{d\tau}. \quad (4)$$

Thus the voltage  $V_n$  across the  $n^{\text{th}}$  unit is given by

$$V_n = V_C + V_L + V_R = \frac{q_n}{C_0} + a_3 q_n^3 - R_0 i_0 \left( \frac{i_n}{i_0} - \left(\frac{i_n}{i_0}\right)^3 \right) - L \frac{di_n}{d\tau} \quad (5)$$

where  $q_n$  is the charge on its nonlinear capacitor and  $i_n$  the current through all three elements.

With free ends,  $i_n = 0$  and  $q_n$  is constant, so nothing happens. Each unit becomes a self-exciting oscillator if its ends are connected, however because the equation  $i_n = 0$  is replaced by  $V_n = 0$ , which combined with (2) is a second-order nonlinear differential system, and standard phase plane analysis [22] shows there is an unstable equilibrium at  $q_n = 0, i_n = 0$  surrounded by an attracting limit cycle

(if  $a_3$  is very negative this conclusion requires the previously mentioned addition of a term to keep  $V_C$  of the same sign as  $q$ ).

An alternative way to view each unit as a self-exciting oscillator, more natural in this context, is to connect each of its ends to ground via a capacitor of value  $C_m/2$  as in Figure 2(b). Then writing  $U_{\pm}$  for the voltages across the capacitors  $C_m/2$  at the left and right respectively, and  $q_{\pm}$  for their charges, we obtain

$$\frac{dq_{\pm}}{d\tau} = \mp i, \quad U_{\pm} = \frac{2q_{\pm}}{C_m}, \quad V_n = U_+ - U_-. \quad (6)$$

The first equation in (6) implies that  $q_{\pm} = c_{\pm} \mp q$  for some constants  $c_{\pm}$ , and thus the second and third lead to  $V_n = \frac{2}{C_m}(c_+ - c_-)$ . We suppose that  $c_{\pm} = 0$ , corresponding to there being no initial imbalance of charge in the circuit, and thereby recover the equation  $V_n = 0$  for the case with the ends connected.

The ring of Figure 1 is obtained by joining neighbouring ends of units of Figure 2(a) to a capacitor  $C_m$  to ground, (equivalently just joining the units of Figure 2(b) at the tops of neighbouring capacitors  $C_m/2$ ). Denoting the voltage at the left end of the  $n^{\text{th}}$  unit by  $U_n$  and identifying  $n = 0$  with  $n = N$ , we obtain

$$i_n - i_{n-1} = -C_m \frac{dU_n}{d\tau}, \quad U_{n+1} - U_n = V_n. \quad (7)$$

Combining the first equation of (7) with (2) we obtain  $U_n = (q_{n-1} - q_n)/C_m + c_n$  for some constants  $c_n$ , which we again take to be zero corresponding to no initial charge imbalance. Then using equation (2) again, the second equation of (7) yields

$$L \frac{d^2 q_n}{d\tau^2} - R_0 \left[ 1 - \frac{1}{i_0^2} \left( \frac{dq_n}{d\tau} \right)^2 \right] \frac{dq_n}{d\tau} + \frac{q_n}{C_0} + a_3 q_n^3 = \frac{1}{C_m} (q_{n+1} - 2q_n + q_{n-1}),$$

$$n = 1, 2, \dots, N \text{ mod } N.$$

Putting  $\omega_e^2 = \frac{1}{LC_0}$  and introducing the dimensionless variables  $x_n = \frac{\omega_e}{i_0} q_n$ ,  $t = \omega_e \tau$  and parameters

$$\mu = \frac{R_0}{L\omega_e}, \quad \beta = \frac{a_3 i_0^2}{L\omega_e^4}, \quad K = \frac{C_0}{C_m},$$

equation (8) yields the following set of coupled non-dimensional differential equations

$$\ddot{x}_n - \mu(1 - \dot{x}_n^2)\dot{x}_n + x_n + \beta x_n^3 = K(x_{n+1} - 2x_n + x_{n-1}), \quad n = 1, 2, \dots, N. \quad (8)$$

We introduce  $y_n = \dot{x}_n$  (a non-dimensionalisation of  $i_n$ ) to obtain

$$\begin{aligned} \dot{x}_n &= y_n, \\ \dot{y}_n &= \mu(1 - y_n^2)y_n - x_n - \beta x_n^3 + K(x_{n+1} - 2x_n + x_{n-1}), \quad n = 1, 2, \dots, N. \end{aligned} \quad (9)$$

The equations (9) are a set of  $N$  mutually coupled identical *Rayleigh-Duffing* equations. As mentioned in the introduction, this system can model rings of microwave oscillators which produce high power if synchronised.

### 3. Stability theory for synchronous solutions.

In the context of a network of identical units, as here, we say a solution is *synchronous* if all units have identical time dependence. As mentioned in the introduction, this system can model systems of microwave oscillators which produce high power if synchronised. Equivalently they lie on the *synchronization sub-manifold* [19]  $\mathcal{S} = \{x_1 = x_2 = \dots = x_N, y_1 = y_2 = \dots = y_N\}$ . It has dimension two, that of a single

unit. It is invariant under the dynamics by the assumption of shift-invariance of the ring, and the dynamics on  $\mathcal{S}$  is that of a single unit because the coupling has no effect there. The behavior on  $\mathcal{S}$  is limited by the Poincaré-Bendixson theorem [20], so the interest focusses on periodic solutions.

The central goal of this investigation is to predict when a synchronized periodic solution  $x_n = x_s(t)$ ,  $y_n = y_s(t)$ ,  $\forall n$  is stable. The linear stability of the resulting dynamical states can be determined by letting  $x_n = x_s + X_n$ ,  $y_n = y_s + Y_n$  and linearizing equations (9) around the solution  $(x_s, y_s)$ . This leads to

$$\begin{aligned}\dot{X}_n &= Y_n \\ \dot{Y}_n &= \mu(1 - 3y_s^2)Y_n - (1 + 3\beta x_s^2)X_n + K(X_{n+1} - 2X_n + X_{n-1}),\end{aligned}\quad (10)$$

Since the system has translation symmetry, the variational equations (10) can be block-diagonalised by transforming to spatial *Fourier* modes  $(\xi_k, \eta_k)$  [19, 21] defined by

$$\begin{aligned}X_n &= \frac{1}{\sqrt{N}} \sum_{k=0}^{N-1} \xi_k \exp(-2\pi ink/N), \\ Y_n &= \frac{1}{\sqrt{N}} \sum_{k=0}^{N-1} \eta_k \exp(-2\pi ink/N).\end{aligned}\quad (11)$$

The variational equations (10) take the form

$$\begin{aligned}\dot{\xi}_k &= \eta_k, \\ \dot{\eta}_k &= \mu(1 - 3y_s^2)\eta_k - \left\{ 1 + 3\beta x_s^2 + 4K \sin^2 \left\{ \frac{\pi k}{N} \right\} \right\} \xi_k, \\ k &= 0, 1, \dots, N - 1.\end{aligned}\quad (12)$$

The mode  $k = 0$  represents the linearized equations tangent to  $\mathcal{S}$ . The remaining variations  $(\xi_k, \eta_k)$ ,  $k = 1, 2, \dots, N - 1$  are transverse to  $\mathcal{S}$ , and describe the system's response to small deviation from the synchronization manifold.

The stability of the synchronized state is ensured if arbitrary small transverse variations from the synchronization manifold decay to zero as  $t \rightarrow +\infty$ . Therefore, a necessary condition for the stability of the synchronous state is that all the transverse ( $k \geq 1$ ) *Lyapunov* exponents be non-positive i.e  $\lambda_j^k \leq 0$ . If some *Lyapunov* exponent is positive, then the corresponding transverse modes are unstable, and there will be no stable synchronization (US). On the other hand, if all *Lyapunov* exponents are negative, the transverse modes  $k$  are stable, then stable synchronization (SS) will occur from initial conditions sufficiently close to the synchronization manifold. If some transverse Lyapunov exponent is zero and none are positive then nonlinear analysis is required to assess the stability of synchronisation.

Before continuing with this analysis, it is worth noting that although  $(\xi_k, \eta_k)$  are in general complex, their real and imaginary parts satisfy the same equations, so only the equations  $k = 1, \dots, \frac{N}{2}$  need to be considered to decide the stability of the synchronous state. This is also understood by the even symmetry of the term  $\sin^2(\pi k/N)$  in equation (12), or from a mathematical perspective by the dihedral  $D_N$  symmetry (including reflections in the ring as well as translations). The highest wave number (shortest wavelength) mode occurs at  $k_{max} = N/2$ .

We now proceed to develop some qualitative theory for a general version of the linearized equations (12) about a synchronous solution. They take the form

$$\begin{aligned}\dot{\xi} &= \eta, \\ \dot{\eta} &= (f(t) - c)\xi + g(t)\eta,\end{aligned}\tag{13}$$

where  $c = 4K \sin^2(\pi k/N)$ ,  $f(t) = -(1 + 3\beta x^2(t))$ ,  $g(t) = \mu(1 - 3y^2(t))$ . These can be written in matrix form as

$$\dot{\zeta} = L_c(t)\zeta,\tag{14}$$

with

$$\zeta = \begin{bmatrix} \xi \\ \eta \end{bmatrix}, \quad L_c(t) = \begin{bmatrix} 0 & 1 \\ f(t) - c & g(t) \end{bmatrix}.$$

Attention will be restricted to the case when the synchronized solution is an attracting periodic orbit. Denote its period by  $T$ .

Stability of the synchronized solution is determined mainly by the *Floquet multipliers*, i.e. the eigenvalues  $\mu_1^k, \mu_2^k$  of the monodromy matrices  $M_k(T)$ , where  $M_k(t)$  is the matrix solution of

$$\dot{M} = L_c(t)M,\tag{15}$$

starting from  $M(0) = I$  (the identity), for  $c = 4K \sin^2(\pi k/N)$  with  $k = 0, \dots, N-1$ . In particular, if there is a Floquet multiplier  $\mu_j^k$  with  $|\mu_j^k| > 1$  then the reference solution is unstable; if all Floquet multipliers apart from a simple one at +1 (corresponding to phase shift) satisfy  $|\mu_j^k| < 1$  then the solution is stable (and attracting).

Writing

$$M_k(T) = \begin{bmatrix} A & B \\ C & D \end{bmatrix}\tag{16}$$

then  $\mu_j^k = \frac{A+D}{2} \pm \sqrt{\frac{(A-D)^2}{4} + BC}$ . For numerical accuracy it is better to compute  $\mu_1^k = \frac{A+D}{2} + \text{sign}(A+D)\sqrt{\frac{(A-D)^2}{4} + BC}$  and  $\mu_2^k = \frac{AD-BC}{\mu_1}$  and compute  $\Delta = AD - BC$  by the formula after (19) below, which avoids large cancellation and resulting numerical noise.

Instead of the Floquet multipliers, it is often convenient to use the Lyapunov exponents  $\lambda_j^k$ . They can be derived from the Floquet multipliers by

$$\lambda_j^k = \frac{1}{T} \log |\mu_j^k|.\tag{17}$$

The solution is unstable if it has a positive Lyapunov exponent; it is stable (and attracting) if all its Lyapunov exponents except for a simple one at 0 are negative.

For  $c = 0$  the linearized equations are simply those for a single oscillator. Thus there is one Floquet multiplier +1 corresponding to phase shift along the orbit. The orbit for a single oscillator is assumed to be linearly attracting, thus the other Floquet multiplier is inside the unit circle.

The product of the Floquet multipliers for given  $c$  is equal to the determinant of  $M(T)$ . The determinant  $\Delta(t)$  of  $M(t)$  evolves from  $\Delta(0) = 1$  by

$$\dot{\Delta} = \text{tr} L_c(t)\Delta.\tag{18}$$

Thus  $\Delta(T) = \exp \int_0^T \text{tr} L_c(t) dt$ . Since  $\text{tr} L_c(t) = g(t)$  is independent of  $c$ ,  $\Delta(T)$  is for all  $c$  equal to its value for  $c = 0$ ; this is just the second Floquet multiplier for a single oscillator. Let  $\lambda_{max}^k = \max_{(j=1,2)} \lambda_j^k$ . Then  $\lambda_{max}^k$  is given by evaluating the largest Lyapunov exponent of (15), named the master stability function in [2], at

$c = 4K \sin^2 \frac{\pi k}{N}$ . Because  $\Delta(T)$  is real and positive, we can write the second Floquet multiplier as  $e^{-\nu T}$ , with

$$-\nu = \frac{1}{T} \int_0^T g(t) dt$$

denoting the second Lyapunov exponent for a single oscillator. It follows that for all  $c$ , the product of the Floquet multipliers is  $e^{-\nu T}$ . In particular for all  $c$ ,

$$\lambda_1^k + \lambda_2^k = -\nu. \quad (19)$$

If the Floquet multipliers are complex or a repeated real, then they have equal modulus and so the Lyapunov exponents are equal. Thus by the above, they both equal  $-\nu/2$ . If they are distinct reals then (19) determines only their sum. So we can expect the graph of the Lyapunov exponents against  $c$  to have intervals where both equal  $-\nu/2$ , alternating with intervals where they differ (but average to  $-\nu/2$ ).

#### 4. Prüfer transformation and consequences.

To understand further qualitative features of how the Lyapunov exponents depend on  $c$ , it is convenient to transform to polar coordinates  $(r, \theta)$  in the  $(\xi, \eta)$ -plane, known as Prüfer variables in Sturm-Liouville theory [22]. The Lyapunov exponents are given by the growth rate of the radius  $r$ , but  $r$  can be considered as driven by the angular behavior, so we concentrate on the equation for the angle  $\theta$ .

Writing  $\xi = r \cos \theta$ ,  $\eta = r \sin \theta$ , with  $r \geq 0$ , one obtains

$$\dot{\theta} = (f(t) - c) \cos^2 \theta + g(t) \sin \theta \cos \theta - \sin^2 \theta \quad (20)$$

$$\dot{r} = r((1 + f(t) - c) \sin \theta \cos \theta + g(t) \sin^2 \theta). \quad (21)$$

These equations are equivariant with respect to adding any multiple of  $\pi$  to  $\theta$ . Since the synchronized solution has period  $T$ , they are also periodic in  $t$  with period  $T$ . In the case of odd nonlinearity they actually have period  $T/2$ , but discussion of the consequences is deferred to later in this section.

Since the plane of  $(t, \theta)$  is two-dimensional, solutions of (20) for given  $c$  can not cross each other. In particular, no solution can cross any of its translates by multiples of  $\pi$  in  $\theta$  or  $T$  in  $t$ , so (as proved by Poincaré, e.g. [20]) the average rotation rate  $\rho = \lim_{t \rightarrow \infty} \frac{\theta(t) - \theta(0)}{t}$  of a solution is well defined. Secondly, if one solution has an average rotation rate  $\rho$  then so do all; denote the common value by  $\rho(c)$ .

For  $c = 0$  the angle of the tangent to the synchronized solution in the  $(x, y)$ -plane is a solution. For the example studied, the tangent turns once clockwise in one period, so  $\rho(0) = -\frac{2\pi}{T}$ .

Since  $\cos^2 \theta \geq 0$ , for any two values  $c_1 < c_2$  of  $c$ , solutions for  $c_2$  in the plane of  $(t, \theta)$  can not cross upwards those for  $c_1$ . Thus the average rotation rate  $\rho(c)$  is non-increasing with respect to  $c$ . It depends continuously on  $c$  by an argument of Poincaré [20]: given  $c_0$ , for any integer  $n > 0$ , there is a neighbourhood  $U$  of  $c_0$  such that for all  $\theta(0)$ , the change in  $\theta(T)$  for changing  $c_0$  to  $c \in U$  is less than  $\pi/n$  in absolute value. Thus the change in  $\theta(nT)$  is less than  $\pi$ . If  $\rho(c_0) < m\pi/nT$  for some integer  $m$ , it follows that  $\rho(c) < (m+1)\pi/nT$  for all  $c \in U$ . Similarly, if  $\rho(c_0) > m\pi/nT$  then  $\rho(c) > (m-1)\pi/nT$ . So the rotation rate can change by at most  $2\pi/nT$ .

The rotation rate is non-positive for all  $c$ , because when  $\theta = \pi/2$  then  $\dot{\theta} = -1$ , so all trajectories cross  $\theta = \pi/2$  (and all translates by multiples of  $\pi$ ) downwards.

If  $\rho$  is not a multiple of  $\pi/T$  then the Floquet multipliers are complex (and so the Lyapunov exponents are equal to  $-\nu/2$ ). This is because to have a real

Floquet multiplier,  $M(T)$  must have a real eigenvector. Its direction gives an initial condition  $\theta(0)$  such that  $\theta(T)$  is in the same or opposite direction, meaning it differs by a multiple  $m$  of  $\pi$ . Thus  $\rho = m\pi/T$ .

Conversely, if  $\rho$  is a multiple of  $\pi/T$  then the Floquet multipliers are real, because for  $\rho = m\pi/T$  there is a period- $T$  orbit of the  $\theta$  equation (modulo  $\pi$ ): take as initial condition the limit of  $\theta(nT) - nm\pi$  as  $n \rightarrow \infty$  from an arbitrary  $\theta(0)$  (this sequence is monotone and bounded so converges). A period- $T$  orbit for  $\theta$  implies a real eigenvector in that direction for  $M(T)$ , with real eigenvalue. Since there are only two Floquet multipliers, if one is real so is the other.

More generally, the arguments of the Floquet multipliers in the complex plane are those of  $e^{\pm i\rho T/2\pi}$ .

If for some value of  $c$  there is a non-degenerate period- $T$  orbit for  $\theta$  (meaning its linearized time- $T$  map has eigenvalue not equal to  $+1$ ), then the same is true for all nearby values of  $c$ . Thus the rotation rate is constant at a value  $\rho = m\pi/T$  until values of  $c$  for which all period- $T$  orbits are degenerate.

Furthermore, if there is a non-degenerate period- $T$  orbit then the Lyapunov exponents are distinct because the linearisation of equation (20) is

$$\delta\dot{\theta} = q(t, \theta) \delta\theta \quad (22)$$

with

$$q(t, \theta) = g(t) (\cos^2 \theta - \sin^2 \theta) - 2(1 + f(t) - c) \sin \theta \cos \theta, \quad (23)$$

so the eigenvalue for its time- $T$  map is  $\kappa = \exp \int_0^T q(t, \theta(t)) dt$ , and the equation (21) for  $r$  can be written as

$$\frac{\dot{r}}{r} = \frac{g}{2} - \frac{q(t, \theta)}{2}. \quad (24)$$

Thus the non-degenerate period- $T$  orbit of (20) gives a Lyapunov exponent for the original system

$$\lambda = \frac{1}{T} \int_0^T \left[ \frac{1}{2}g(t) - \frac{1}{2}q(t, \theta) \right] dt = -\frac{\nu}{2} - \frac{1}{2T} \log \kappa. \quad (25)$$

Since we assumed non-degeneracy,  $\kappa \neq 1$  and thus  $\lambda \neq -\nu/2$ . The sum of the Lyapunov exponents is  $-\nu$  so since one is not  $-\nu/2$  then they are distinct.

Generically the rotation rate can not cross an integer multiple of  $\pi/T$  as  $c$  varies without locking to that integer multiple for an interval of  $c$ . This is because the only way for  $\rho(c)$  to cross immediately from above to below  $m\pi/T$  is that every orbit of the  $\theta$  flow have period  $T$  at the transition case. This implies that  $M(T)$  is a multiple of the identity, a phenomenon of codimension 3, so unlikely in a 1-parameter family. On the other hand, it can be forced to happen if there are additional symmetries. In particular, if  $f$  and  $g$  are even, as is the case for oscillators with odd nonlinearity, then (20) has period  $T/2$  in  $t$ , and it follows that  $M(T)$  is the square of the matrix  $M(T/2)$ , so is a negative multiple of the identity whenever the arguments of the eigenvalues of  $M(T/2)$  pass through  $\pm\pi/2$  (then  $M(T/2)$  is conjugate to a scalar multiple of a rotation by  $\pi/2$ ).

Generically, the rotation rate changes like a square root with respect to  $c$  at the ends of a step, and the Lyapunov exponents separate like a square root inside the step. These statements can be proved by unfolding the case with a degenerate period- $T$  orbit under the codimension-3 assumption that  $M(T)$  is not a multiple of the identity. Then  $M(T)$  is a multiple of a shear and there is a unique period- $T$



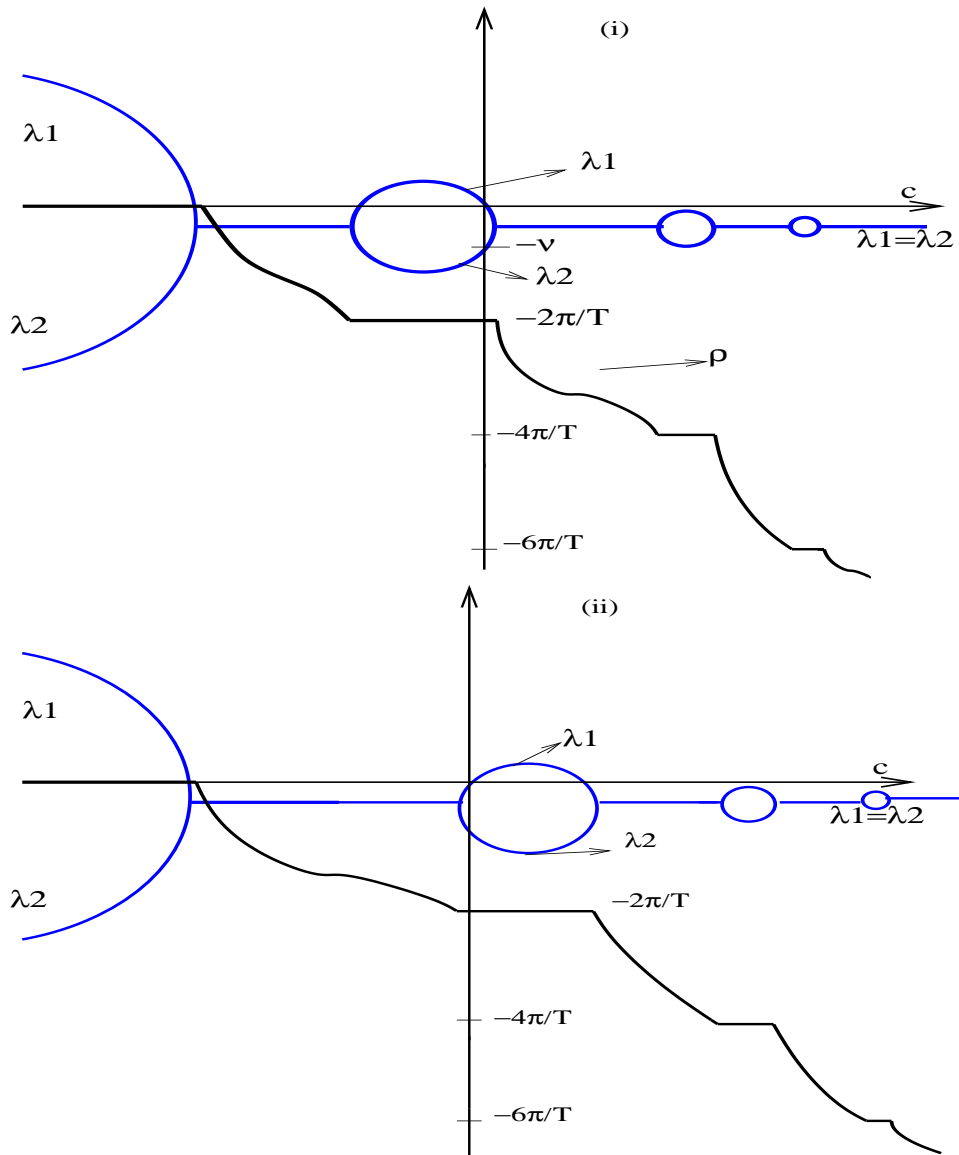


FIGURE 3. Sketch of expected behavior of rotation rate and Lyapunov exponents as functions of  $c$  for (i)  $\lambda'(0) < 0$ , e.g.  $\beta$  sufficiently positive (hardening), and (ii)  $\lambda'(0) > 0$ , e.g.  $\beta$  sufficiently negative (softening).

orbit. It can be checked that the quadratic term in the expansion of the time- $T$  map for  $\theta$  is non-zero, and that changing  $c$  crosses this case transversely.

For values not a multiple of  $\pi/T$  the rotation rate  $\rho$  is a differentiable function of  $c$  with negative derivative. A proof is given in Appendix A. For  $f$  and  $g$  of period  $T/2$  the result of Appendix A can be applied to the time  $T/2$ -map and thus the conclusion also holds for all values of  $\rho$  not a multiple of  $2\pi/T$ .

If  $c \leq \min_t f(t)$  then  $\dot{\theta} \geq 0$  at  $\theta = 0$ , thus the strip  $0 \leq \theta \leq \pi/2$  is forward invariant and so  $\rho(c) = 0$ . In particular, the Floquet multipliers are real.

On the other hand,  $\rho(c) \rightarrow -\infty$  as  $c \rightarrow +\infty$ , because for  $c$  large and positive,  $\theta$  decreases by  $\pi$  in a time less than the function  $\tau(c)$  given by replacing  $f$  by its maximum and  $g \sin \theta \cos \theta$  by the maximum of  $g$ . The function  $\tau(c)$  is positive and goes to zero as  $c$  goes to infinity, so  $\rho(c) \leq -\pi/\tau(c) \rightarrow -\infty$ .

When the Floquet multipliers are distinct, they depend differentiably on  $c$  (the monodromy matrix depends analytically on  $c$  by standard ODE theory, and simple eigenvalues of a matrix depend as smoothly on parameters as the matrix does by applying the implicit function theorem to the eigenvalue-eigenvector problem with a normalization condition on the eigenvector). Thus the Lyapunov exponents depend smoothly on  $c$  whenever they are distinct.

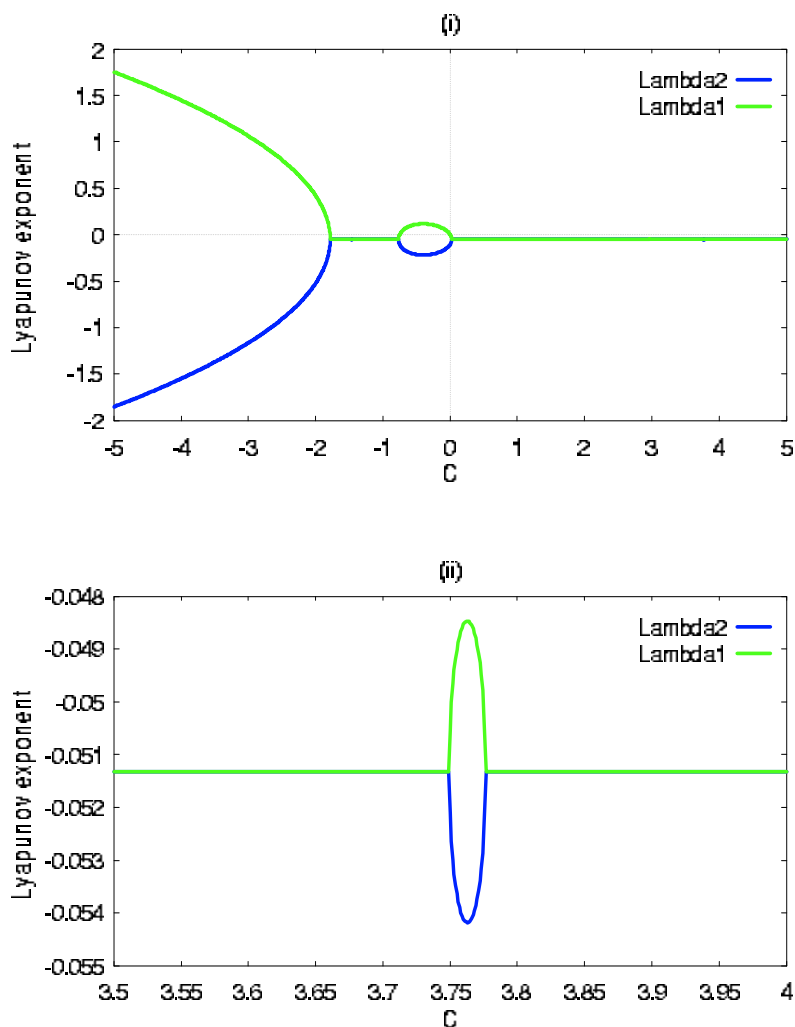


FIGURE 4. Variation of the Lyapunov exponents versus the coupling coefficient  $c$  for the case  $\mu = 0.1$ ;  $\beta = 0.5$ .

The remaining question is for what subset, if any, of  $c$  in each step for the rotation rate function is there a positive Lyapunov exponent? We begin with the  $\rho = 0$  step. For  $c$  large and negative, one of the Lyapunov exponents is positive, and in fact grows asymptotically like  $\sqrt{|c|}$ . One way to see this is to use (26). For  $c$  large and negative there is a period- $T$  orbit of the  $\theta$  equation close to  $\theta_0 = \cot^{-1}(\sqrt{|c|})$ , because one can use the implicit function theorem to find a nearby zero of the map from  $C^1$  functions of period- $T$  to  $C^0$  functions of period- $T$  defined by  $\theta \mapsto c \cos^2 \theta + \sin^2 \theta + (\epsilon \dot{\theta} - f \cos^2 \theta + g \sin \theta \cos \theta)$  for  $\epsilon \in [0, 1]$ . Then (26) gives

$$\lambda = -\frac{\nu}{2} - \frac{1}{2T} \int_0^T [g(t) \cos 2\theta - (1 + f - c) \sin 2\theta] dt = \sqrt{|c|} + O(1) \text{ as } c \rightarrow -\infty, \quad (26)$$

using  $\theta(t) \approx \theta_0$  and  $\int_0^T g(t) dt = -\nu T$ .

For the steps with  $\rho = -2\pi m/T$ ,  $m$  large, equivalently  $c$  large and positive, put  $\tilde{\eta} = \eta/\sqrt{c}$ ,  $\tau = \sqrt{c}t$ ,  $\tilde{\xi} = \xi$ ,  $\tilde{\zeta} = (\tilde{\xi}, \tilde{\eta})$ , to obtain

$$\frac{d\tilde{\zeta}}{d\tau} = \begin{bmatrix} 0 & 1 \\ -1 + \frac{f(t)}{c} & \frac{g(t)}{\sqrt{c}} \end{bmatrix} \tilde{\zeta} \quad (27)$$

for  $\tau = 0$  to  $\sqrt{c}T$ . Because the dominant dynamics is rotation at rate 1 over a long interval in  $\tau$  with  $f$  and  $g$  slowly and smoothly varying, there is an averaging effect which renders the monodromy matrix in these coordinates within  $1/\sqrt{c}$  of that given by replacing  $g$  by its average ( $-\nu$ ) and  $f$  by  $-\nu^2/4$ . The resulting approximation is conjugate to  $e^{-\nu T/2}$  times a rotation. Thus as the corrections are turned on,  $M(T) \pm I$  remains invertible for  $c$  large enough, hence no Floquet spectrum can cross the unit circle, and so no Lyapunov exponent becomes positive.

For the  $\rho = -2\pi/T$  step, we know that  $\lambda_1 = 0$  at  $c = 0$  so if the slope  $d\lambda_1/dc$  is non-zero then  $\lambda_1$  is positive for one sign of small  $c$ . To decide for which sign of small  $c$  we have  $\lambda_1 > 0$ , the following formula for  $\lambda' = d\lambda_1/dc$  at  $c = 0$  was obtained:

$$\lambda'(0) = -\frac{1}{T} \int_0^T B_2(t) \dot{x}(t) dt, \quad (28)$$

where  $B_2(t)$  is the second component of the linear functional  $B(t)$  measuring phase shift for linearised displacements from the limit cycle. More specifically, let  $(\xi, \eta)(t)$  be a non-zero solution of the linearised equations about the synchronised solution corresponding to Floquet multiplier  $e^{-\nu T}$ . Then any tangent vector  $v$  at  $(x, y)(t)$  can be written uniquely as  $(a\dot{x}(t) + b\xi(t), a\dot{y}(t) + b\eta(t))$  for some  $(a, b)$ , and  $B(t)v = a$ . A proof of (28) is given in Appendix B.

So the sign of  $\lambda'(0)$  is determined by averaging  $B_2(t)\dot{x}(t)$  round the limit cycle. Although it is amenable to numerical computation, its sign is not transparently clear to us. Nonetheless, the following qualitative analysis allows us to determine its sign when the basic oscillator is sufficiently anharmonic.

If the basic oscillator is sufficiently hardening, meaning that the trajectories of initial conditions outside the limit cycle rotate significantly faster than those on the limit cycle (as for  $\beta$  sufficiently positive), then the  $\rho = -2\pi/T$  step extends only a short way on the  $c > 0$  side, and leads to no instability on that side and an interval  $(c_-, 0)$  of instability on the  $c < 0$  side. To see this, the hardening assumption implies that any initial angle  $\theta(0) \in (-\frac{\pi}{2}, \frac{\pi}{2} - )_\epsilon$  of tangent vector at the intersection of the limit cycle with the positive  $x$ -axis for some  $\epsilon > 0$  small, is attracted close to the orbit for  $\theta(0) = -\frac{\pi}{2}$  when  $c = 0$ . So the repelling period- $T$  orbit is just below the attracting one in the  $(t, \theta)$ -plane. Then making  $c > 0$  pushes

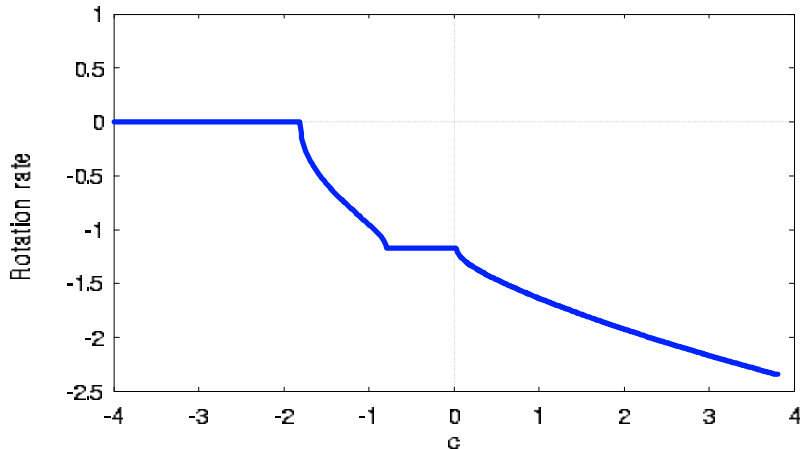


FIGURE 5. Variation of the rotation rate  $\rho$  versus the coefficient  $c$  for the case  $\mu = 0.1; \beta = 0.5$ .

the two period- $T$  orbits towards each other and they annihilate at a small positive value of  $c$ . This bifurcation corresponds to the right hand end of the  $\rho = -2\pi/T$  step and thus the Lyapunov exponents equal  $-\nu/2$  there and separate like a square root as  $c$  decreases.

If on the other hand the basic oscillator is sufficiently softening, meaning that the trajectories of initial conditions outside the limit cycle rotate significantly slower than those on the limit cycle (as for  $\beta$  sufficiently negative), then a similar argument shows that the  $\rho = -2\pi/T$  step extends only a short way on the  $c < 0$  side, the Lyapunov exponents are negative for all negative  $c$  in the step and there is an interval  $(0, c_+)$  of instability on the positive side.

The conclusion is that for a system with odd symmetry in  $(x, y)$ , the Lyapunov exponents as a function of  $c$  should behave like Figure 3 (i) or (ii); the behavior of the rotation rate  $\rho$  is also sketched. Case (i) is expected if the dynamics of a single unit is sufficiently *hardening*; while case (ii) if sufficiently *softening*. If odd symmetry is not assumed there should be additional steps at rotation rate equal to odd multiples of  $\pi/T$  and associated bubbles of distinct Lyapunov exponents.

## 5. Numerical study.

Now we report on numerical computation of the Lyapunov exponents and some simulations of the dynamics. For this purpose, a fourth-order *Runge-Kutta* algorithm was used to solve the equations of motion with the set of the parameters  $\mu = 0.1$  and  $\beta = 0.5$  or  $-0.1$ . The analysis after equation (28) leads us to expect that these two cases have  $\lambda'(0)$  negative and positive, respectively, and the numerics will be seen to confirm this. For intermediate  $\beta$  one can expect a transition between the two cases at some  $\beta_c$  for which  $\lambda'(0) = 0$ ; at  $\beta_c$  it is likely that  $\lambda(c) < 0$  for both signs of small  $c$ , giving rise to enhanced stability domains for synchronisation.

### 5.1. Case $\beta = 0.5$ .

In this subsection, we study the case  $\beta = 0.5$ , which is a quite strongly hardening nonlinearity so can be expected to lead to  $\lambda'(0) < 0$ . When the coupling coefficient is turned off (i.e  $K$  is equal to zero), the Lyapunov exponents are  $\lambda_1^0 = 0$ ,  $\lambda_2^0 = -\nu \approx -0.1$ . For  $K \neq 0$ , and for a given value of  $N$ , the Lyapunov exponents will

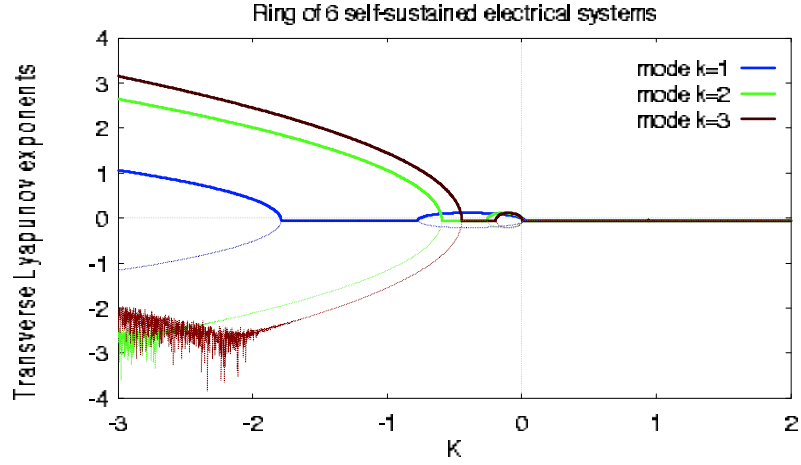


FIGURE 6. Variation of the transverse Lyapunov exponents versus the coupling coefficient  $K$  of a ring of 6 self-sustained electrical units for the case  $\mu = 0.1; \beta = 0.5$ .

enable us to derive the range of the coupling parameter  $K$  in which the transverse Fourier modes are stable, and then each system in the ring of mutually self-sustained electrical systems can work synchronously. By the preceding theory, they are given by evaluating the Lyapunov exponents for (13) at values of  $c = 4K \sin^2 \frac{\pi k}{N}$ . The functions  $f$  and  $g$  are determined from a numerical solution for  $(x_s, y_s)$  from the equations of motion (9).

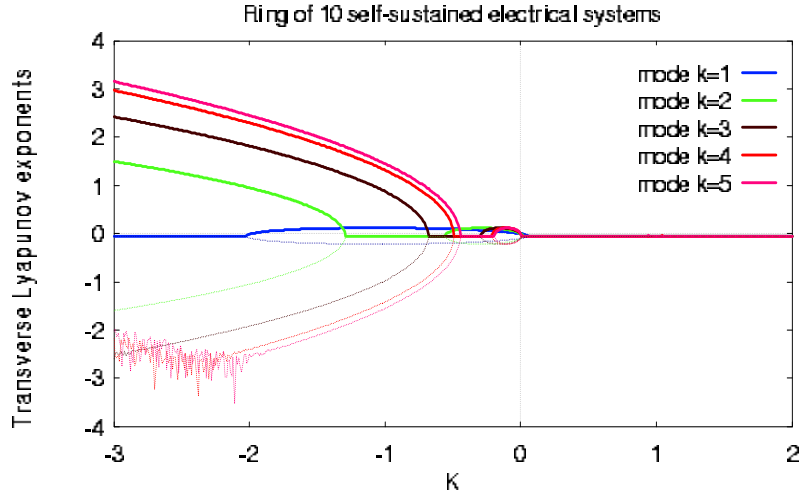


FIGURE 7. Variation of the transverse Lyapunov exponent versus the coupling coefficient  $K$  of a ring of 10 self-sustained electrical units for the case  $\mu = 0.1; \beta = 0.5$ .

The dependence of the Lyapunov exponents with  $c$  is plotted on Figure 4. Note that the graph is reflection symmetric about the line  $\lambda = -\nu$ , in agreement with (20). As  $c$  increases, consistently with the above analysis, we find the following

domains of dynamical states. First there is the unstable domain in which there is a positive Lyapunov exponent and defined by  $c \in I_{US} = ]-\infty; -1.791[ \cup ]-0.758; 0[$ . Secondly, there is the stable domain, defined as  $c \in I_{SS} = I_{SS-} \cup I_{SS+} = [-1.791; -0.758] \cup ]0; +\infty[$ , where all the Lyapunov exponents are negative. It appears that as  $c$  increases, the Lyapunov exponents are real and distinct with opposite sign until  $c = -1.791$  where the two Lyapunov exponents become both negative, and at  $c = -1.789$  the system passes to an interval of  $c$  where both Lyapunov exponents are equal to  $-\nu/2 \approx -0.051$ . Then at  $c = -0.774$ , a “bubble” for distinct Lyapunov exponents ( $c \in ]-0.774; 0.019[$ ) appears, containing a subinterval  $c \in [-0.758; 0[$  where both Lyapunov exponents are negative, and thereafter the system passes into another domain ( $c > 0.019$ ) with equal Lyapunov exponents (see Figure 4(i)). For larger positive values of  $c$ , we find another bubble in the interval  $c \in [3.75; 3.775]$  with distinct negative Lyapunov exponents (see Figure 4(ii)), but they both remain negative, insufficient to destabilize the ring.

As we expected in the above section, the Lyapunov exponents against  $c$  have intervals where both equal  $-\nu/2$  alternating with intervals where they differ but average to  $-\nu/2$ . Furthermore, the instability near  $c = 0$  is for  $c$  negative, consistent with the expectation that  $\lambda'(0) < 0$ .

Next we plot in Figure 5 the rotation rate  $\rho(c)$  as a function of the parameter  $c$ . The rotation rate is constant at a value  $\rho = -2\pi/T \approx -1.17547$  for the range of  $c$  defined by  $c \in ]-0.774; 0.019[$  and at a value  $\rho \approx 0$  for  $c \in ]-\infty; -1.789[$ . We find in Figure 5 that the rotation rate  $\rho$  decreases and  $\rho(c) \rightarrow -\infty$  as  $c \rightarrow +\infty$ , which is what we expected in section 4.

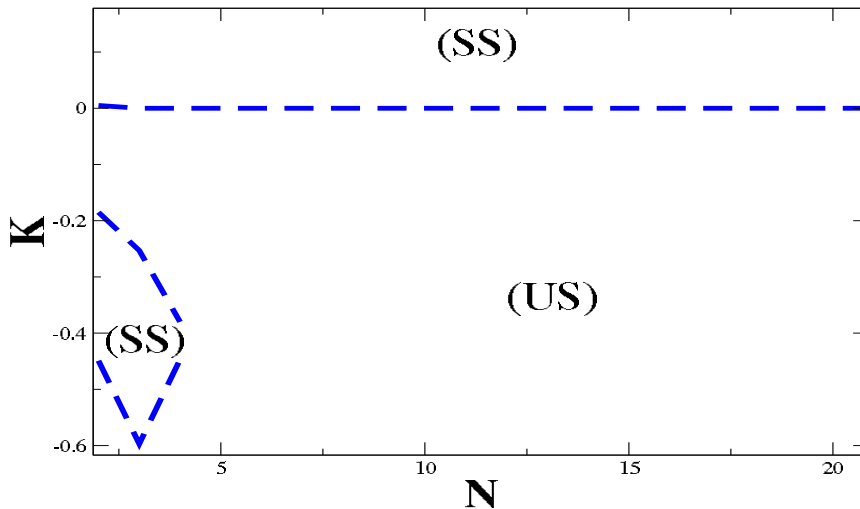


FIGURE 8. The stability diagram of the synchronization process in the  $(N, K)$  plane for the case  $\mu = 0.1; \beta = 0.5$ . (US) Unstable domain and (SS) stable synchronization domain.

After the above analysis which enables us to find the qualitative changes of the Lyapunov exponents and the rotation rate when the parameter  $c$  evolves, we will now use the direct relation between  $c$ , the coupling coefficient  $K$  and the mode  $k$  given by  $K = c/(4 \sin^2(\pi k/N))$  to find the stability of the synchronized state in the ring as the coupling parameter  $K$  varies. The range of  $K$  for unstable synchronization

is derived as  $K \in D_{US}$  is the union over  $k = 1, \dots, N/2$  of  $I_{US}/4 \sin^2(\pi k/N)$ . The variation of the Lyapunov exponents are derived and plotted on Figures 6 and 7 for rings of 6 and 10 mutually coupled self-sustained electrical systems. As  $K$  increases, we find through the above analysis the following domains of dynamical states: The first is the unstable domain in which synchronization is unstable and hardly depends on the number  $N$  as

$$\begin{aligned} D_{US}(N = 4) &= ] - \infty; -0.447[ \cup ] - 0.39; 0[, \\ D_{US}(N > 5) &= ] - \infty; 0[, \end{aligned}$$

In  $D_{US}$  at least one transverse mode is unstable. Secondly, we have the domain of stability  $K \in D_{SS}$ , the complement of  $D_{US}$ ,

$$\begin{aligned} D_{SS}(N = 4) &= ] - 0.447; -0.39[ \cup ] 0; +\infty[, \\ D_{SS}(N > 5) &= ] 0; +\infty[, \end{aligned}$$

In this case, all the transverse modes have negative Lyapunov exponents. Figure 8 displays the stability boundaries. We find that the number of units hardly affects the stability boundaries of the synchronization process in the ring. This is because the relevant values of  $c$  are  $4K \sin^2(k\pi/N)$ , all  $c > 0$  are stable and there is only a short stability interval for  $c < 0$ .

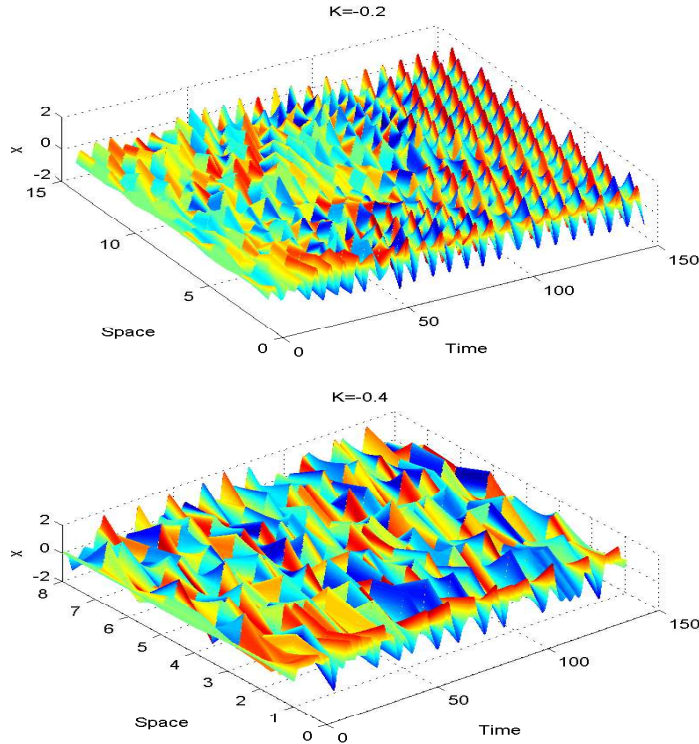


FIGURE 9. *Space-time amplitude plot showing absence of synchronization in the ring for the case  $\mu = 0.1; \beta = 0.5$  and two negative values of  $K$ .*

To illustrate our results, Figures 9 and 10 show space-time amplitude diagrams from simulations of (9) that display behaviors consistent with our analysis for some values of the coupling parameter  $K$  and number  $N$  chosen in the unstable synchronization (US) and stable synchronization (SS) domains. For the unstable domain, Figure 9 shows that for  $(N, K) = (8, -0.4)$  and  $(N, K) = (15, -0.2)$  respectively, no synchronization is found in the ring. Considering the domain of stable synchronization, we confirm in Figure 10 for  $(N, K) = (15, 0.05)$  and  $(N, K) = (8, 0.5)$  that stable synchronization is possible in the ring.

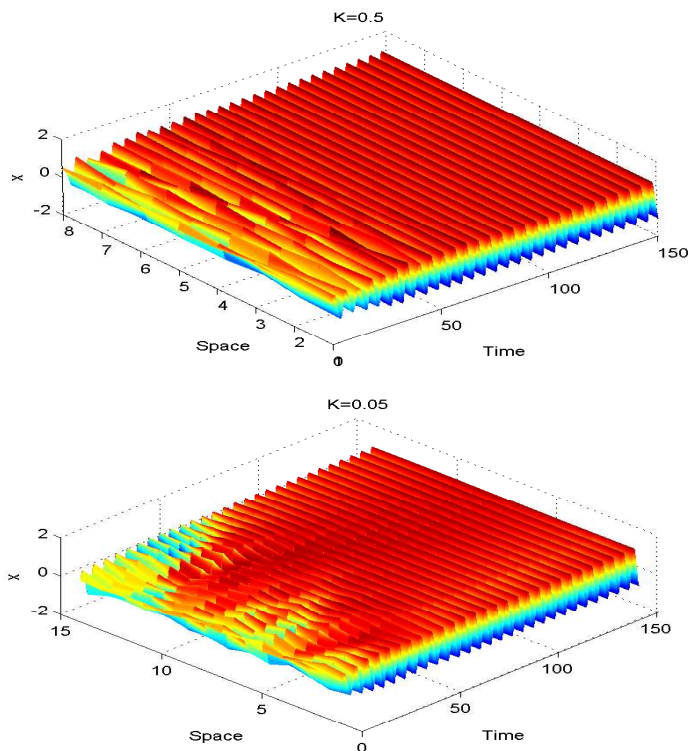


FIGURE 10. Space-time amplitude plot showing convergence to stable synchronization in the ring for the case  $\mu = 0.1; \beta = 0.5$  and two positive values of  $K$ .

## 5.2. Case $\beta = -0.1$ .

Now we study the case  $\beta = -0.1$  which we believe has  $\lambda'(0) > 0$ . It is a softening nonlinearity, but not as large as in the previous subsection, to avoid having to add a term to the model to keep  $V_C$  of the same sign as  $q$  in the range of relevance. The Lyapunov exponents for a single dynamical unit are  $\lambda_1 = 0$ ,  $\lambda_2 \approx -0.051$ . Figures 11 and 12 show respectively the variations of the Lyapunov exponents and the rotation rate  $\rho$  versus  $c$ . As  $c$  increases, we find that the unstable domains are given by  $c \in I_{US} = ]-\infty; -0.83[ \cup ]0; 0.187[$ , while the stable one is given by  $c \in I_{SS} = I_{SS-} \cup I_{SS+} = [-0.83; 0] \cup ]0.187; +\infty[$ . In contrast to the case of a section 5.1, we find that the synchronous solution is unstable for both positive and



negative values of  $c$ , as expected from the qualitative stability theory of section 4. It appears that the rotation rate is constant at a value  $\rho \approx 0$  (for  $c \in ]-\infty; -0.830[$ ) and at  $\rho = -2\pi/T \approx -0.942$  (for  $c \in ]-0.02; 0.26[$ ) corresponding to the intervals where the Lyapunov exponents are distinct. We also find that  $\rho(c) \rightarrow -\infty$  as  $c \rightarrow +\infty$ .

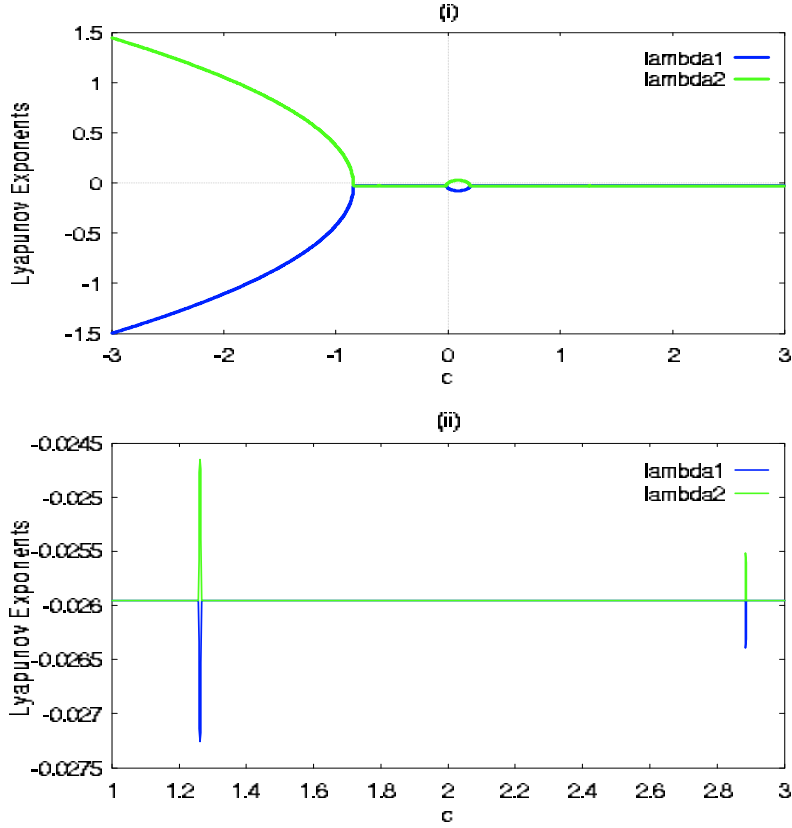


FIGURE 11. Variation of the transverse Lyapunov exponents versus the coupling coefficient  $c$  for the case  $\mu = 0.1; \beta = -0.1$ .

With the above analysis, we find the following dynamical states in the shift-invariant ring. As the number of oscillators in the ring increases, one observes the two main above mentioned dynamical states but for different ranges of  $K$ . For some value of  $N$ , the unstable domains of the synchronization process are:

$$\begin{aligned} D_{US}(N = 4) &= ]-\infty; -0.209[ \cup ]0; 0.094[, \\ D_{US}(N = 10) &= ]-\infty; -0.200[ \cup ]0; 0.500[, \\ D_{US}(N = 15) &= ]-\infty; -0.210[ \cup ]0; 1.090[, \end{aligned}$$

while the stable ones are

$$\begin{aligned} D_{SS}(N = 4) &= [-0.209; 0[ \cup ]0.094; +\infty[, \\ D_{SS}(N = 10) &= [-0.200; 0[ \cup ]0.500; +\infty[, \\ D_{SS}(N = 15) &= ]-0.210; 0[ \cup ]1.090; +\infty[, \end{aligned}$$

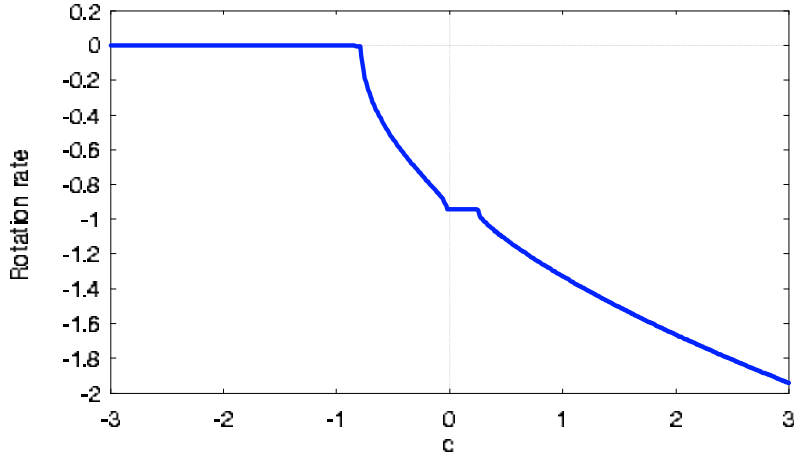


FIGURE 12. Variation of the rotation rate  $\rho$  versus the coefficient  $c$  for the case  $\mu = 0.1$ ;  $\beta = -0.1$ .

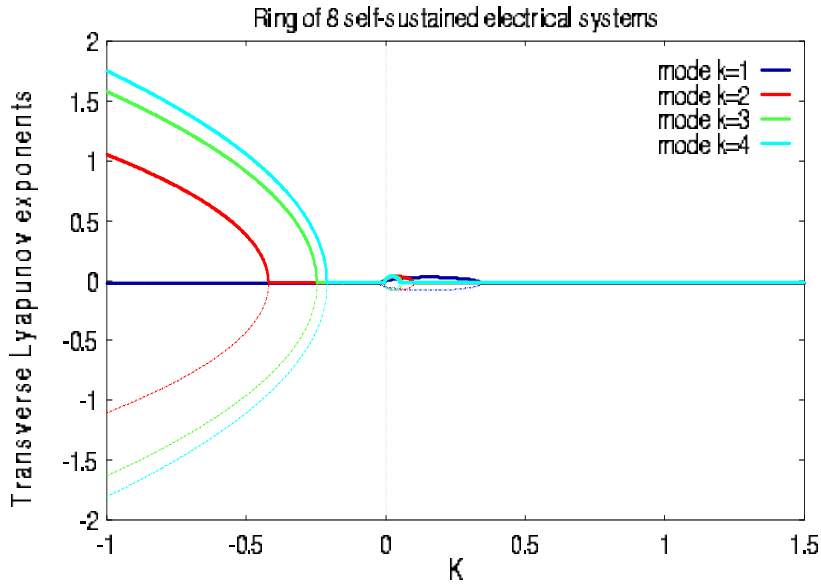


FIGURE 13. Variation of the transverse Lyapunov exponents versus the coupling coefficient  $K$  of a ring in  $N = 6$  self-sustained electrical units for the case  $\mu = 0.1$ ;  $\beta = -0.1$ .

Figures 13 and 14 show the variation of the transverse Lyapunov exponents versus the coupling parameter  $K$  and the regimes of coupling leading to unstable and stable synchronization can be found. Figure 15 shows the stability diagram of the synchronization process in the  $(N, K)$  plane for this case. One can notice that as  $N$  increases, the domain of stable synchronization reduces drastically in the region

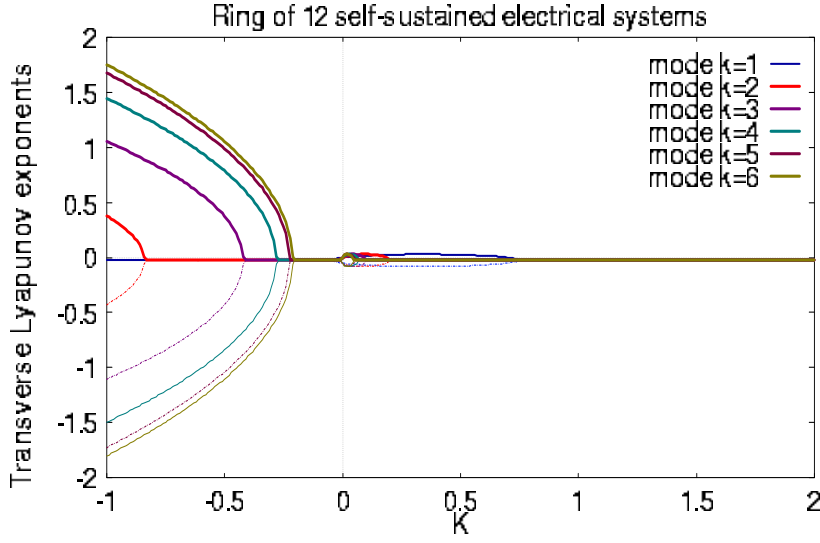


FIGURE 14. Variation of the transverse Lyapunov exponents versus the coupling coefficient  $K$  of a ring of 12 self-sustained electrical units for the case  $\mu = 0.1; \beta = -0.1$ .

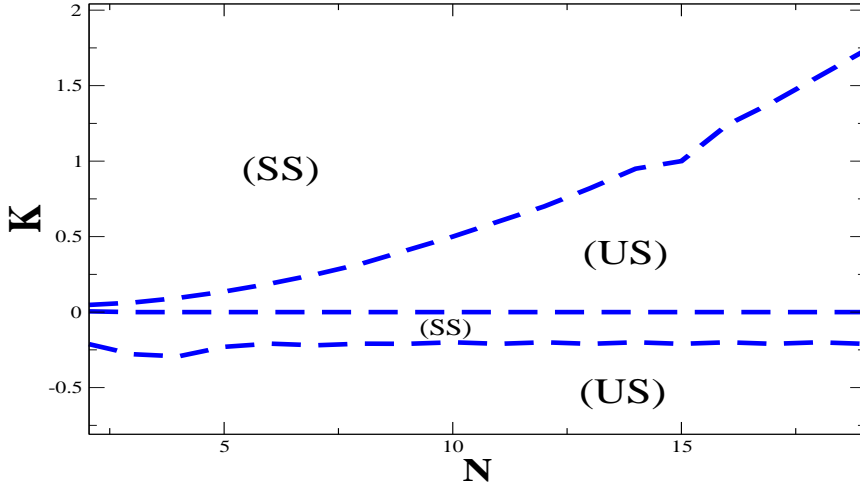


FIGURE 15. The stability diagram of the synchronization process in the  $(N, K)$  plane for the case  $\mu = 0.1; \beta = -0.1$ . (US) Unstable domain and (SS) stable synchronization domain.

of positive  $c$ . This is because as  $N$  increases, the value  $c = 4K \sin^2(\pi/N)$  for mode  $k = 1$  enters the unstable interval for smaller  $K$ .

## 6. Conclusions.

We have studied in this paper the possibility of synchronizing a shift-invariant ring of mutually coupled self-sustained electrical systems. Stability boundaries for

the synchronization process have been derived using the transverse Lyapunov exponents and numerical simulations. They agree with qualitative theory we have developed for the linearized equations about a synchronous solution. A generic feature is that there is a threshold for synchronization for the  $K > 0$  attractive parameter. For  $K < 0$ , the repulsive case, the ring can be synchronized only if the number  $N$  of units is small and  $K$  lies in a special interval of the coupling. The form of the regions of stable synchronisation in  $(N, K)$  space depends crucially on the sign of a quantity  $\lambda'(0)$  defined in (29).

The results extend with only minor change to rings of identical units with certain types of inhomogeneous coupling or more general networks than a ring. For identical units with any linear coupling of the form of a tensor product of a coupling matrix on the network with a fixed matrix on the state space of a single unit, the spatial Fourier decomposition used here generalises to a decomposition into modes of the coupling matrix and the linear stability analysis of a synchronous solution reduces to the same equation (13) but with the parameter  $c$  running over eigenvalues of the coupling matrix [2] (and some extensions to nonlinear coupling are possible [24]). If the coupling matrix is symmetric (or self-adjoint with respect to some inner product) then all the eigenvalues are real and of geometric multiplicity 1; if not then nontrivial Jordan blocks or complex eigenvalues can occur, which require extra treatment (e.g. [25]). For straightforward application of this generalisation, the coupling matrix is assumed to be *balanced*: each of its rows sum to zero; this ensures that a synchronous solution is a solution of an individual unit. This restriction is not necessary for application of our method, however. For an unbalanced coupling matrix the synchronisation submanifold is still of the dimension of a single unit and the equations of motion on it are a small perturbation of those for a single unit if the coupling is small, so the dynamics of a network of self-sustained oscillators can still be expected to give contain synchronous oscillations and one just analyses the one-parameter family of linearised equations about them; one just has to bear in mind that  $c = 0$  is not automatically an eigenvalue of the coupling matrix.

Some directions for future works are: (i) extend the analysis to rings of units of more than two dimensions (this requires analysis of flows on projective spaces of dimension more than 1), (ii) apply the theory of dynamics with dihedral symmetry to deduce some other types of solution, e.g rotating standing waves and analyze their stability, (iii) investigate the extent of the basins of attraction of the stable synchronous solutions, either numerically or by attempting to adapt the method of [23], (iv) for small  $K$ , apply the theory of normally hyperbolic invariant manifold to reduce to a flow on an  $N$ -torus, allow breaking of the dihedral symmetry and study what rotational behavior is possible (in particular, say that two units are synchronized if they have the same average frequency of rotation, and then study what combinations of partial synchrony can occur), (v) study the possible existence and stability of cluster synchronisation.

### Acknowledgements.

This work was done during a visit of R.Yamapi to the University of Warwick from 2 September to 25 November 2006. He thanks the Mathematics Institute for their hospitality and the Royal Society for financial support. We thank the referees for many suggestions leading to improvements.

### Appendix A.

In this appendix it is proved that when the rotation rate  $\rho$  is not a multiple of  $\pi/T$  it is a differentiable function of  $c$  with negative derivative.

Differentiability of  $\rho$  with respect to  $c$  when not a multiple of  $\pi/T$  follows from the relation of  $\rho$  to the argument of a Floquet multiplier given in section 3. When  $\rho$  is not a multiple of  $\pi/T$  the Floquet multipliers are a complex conjugate pair. Simple eigenvalues of a matrix depend as smoothly on parameters as the matrix does. The monodromy  $M(T)$  depends smoothly on  $c$  (in fact analytically). Thus  $\rho$  depends analytically on  $c$  as long as the multipliers are distinct.

We already remarked that the rotation rate is non-increasing with  $c$ , so the derivative is non-positive. To prove that the derivative is negative, we first note that for  $\rho$  not a multiple of  $\pi/T$  the time- $T$  map for equation (20) has an invariant probability measure with positive density. Indeed, it has a unique one of the form

$$d\mu = d\theta / (A + B \sin 2\theta + C \cos 2\theta)$$

on  $\theta \bmod \pi$ , with normalisation condition  $A^2 = \pi^2 + B^2 + C^2$ . To see this, write (20) in the form

$$\dot{\theta} = \alpha + \beta \sin 2\theta + \gamma \cos 2\theta, \quad (29)$$

where  $\alpha = (f - c - 1)/2$ ,  $\beta = g/2$ ,  $\gamma = (f - c + 1)/2$ , and compute that measures of the above form evolve with  $t$  by

$$\frac{d}{dt} \begin{bmatrix} A \\ B \\ C \end{bmatrix} = 2 \begin{bmatrix} 0 & -\gamma & \beta \\ -\gamma & 0 & \alpha \\ \beta & -\alpha & 0 \end{bmatrix} \begin{bmatrix} A \\ B \\ C \end{bmatrix}. \quad (30)$$

The time- $T$  map of (30) is linear and preserves the hyperboloid  $A^2 = \pi^2 + B^2 + C^2$ ,  $A > 0$ . It follows that it is an isometry of the hyperboloid with respect to the standard hyperbolic metric (that induced by restricting the Lorentzian metric  $dA^2 - dB^2 - dC^2$ ). Rotation rate not a multiple of  $\pi/T$  implies the monodromy is conjugate to a rotation, not a multiple of  $\pi$ , so this isometry is elliptic (from which terminology we exclude the identity). Thus it has a unique fixed point. Furthermore, the fixed point (being non-degenerate) depends as smoothly on  $c$  as the coefficients of (29).

Secondly, we note that the time- $T$  map  $f_c$  for the (20) has  $\frac{\partial f}{\partial c}(\theta)$  continuous and negative for all  $\theta$ . This is because by general theory for ODEs the solutions of (20) depend at least as smoothly on  $c$  as  $\dot{\theta}$  depends on  $t, \theta, c$ , and  $\frac{\partial f}{\partial c} = \eta(T)$  where  $\eta$  is the solution from  $\eta(0) = 0$  of

$$\dot{\eta} = q(t, \theta)\eta - \cos^2 \theta,$$

where  $q$  was defined in (23). So

$$\eta(T) = - \int_0^T e^{\int_t^T q \, dt'} \cos^2 \theta(t) \, dt \quad (31)$$

which is non-positive. The only way it could be zero is if  $\theta(t) = \pi/2 \bmod \pi$  for all  $t$ , but  $\dot{\theta} = -1$  whenever  $\theta = \pi/2 \bmod \pi$ , so there is no such possibility.

Thirdly, we prove the following formula for the difference of rotation numbers  $\rho, \tilde{\rho}$  for two lifts of degree-1 circle homeomorphisms  $f, \tilde{f}$  in terms of (lifts of) invariant probability measures  $\mu, \tilde{\mu}$  (the rotation number is the average rate of advance divided by the length of the circle).

**Theorem:**  $\tilde{\rho} - \rho = \int_A d\tilde{\mu}(x) d\mu(x')$ , where  $A$  is the signed area between the graphs  $x' = \tilde{f}(x)$ ,  $x' = f(x)$ , for one period in  $x$  ( $A$  is considered positive where  $\tilde{f}(x) > f(x)$ , negative where  $\tilde{f}(x) < f(x)$ ).

**Proof:** The rotation number  $\rho$  of  $f$  can be written (e.g. [20]) as

$$\rho = \int_x^{f(x)} d\mu(x')$$

for any  $x$  (if  $\mu$  has atoms then use the convention of including them at the lower limit of integration and not the top, for example). This formula can be averaged over  $x$  with respect to any probability measure, in particular  $\tilde{\mu}$  over one period (the period will be denoted by  $\pi$  in keeping with our application). Thus

$$\rho = \int_0^\pi d\tilde{\mu}(x) \int_x^{f(x)} d\mu(x'). \quad (32)$$

This is the  $\tilde{\mu}\mu$  product measure of the signed area between the graph of  $f$  and the diagonal over one period of  $x$ .

Now do the same for the rotation number  $-\tilde{\rho}$  of  $\tilde{f}^{-1}$ :

$$\tilde{\rho} = \int_0^\pi d\mu(x') \int_{\tilde{f}^{-1}(x')}^{x'} d\tilde{\mu}(x).$$

This is the  $\tilde{\mu}\mu$  product measure of the signed region between the graph of  $\tilde{f}$  and the diagonal for one period in  $x'$ . Interchanging the order of integration and using periodicity, it can be rewritten as

$$\tilde{\rho} = \int_0^\pi d\tilde{\mu}(x) \int_x^{\tilde{f}(x)} d\mu(x'),$$

the  $\tilde{\mu}\mu$  measure for one period in  $x$ . Taking the difference gives the required result.

**Corollary 1:** If  $\tilde{f}(x) \geq f(x)$  for all  $x$  with inequality somewhere and  $\mu$  and  $\tilde{\mu}$  have positive densities then  $\tilde{\rho} > \rho$ .

**Proof:**  $\tilde{\mu}\mu$  gives positive measure to the area  $A$ .

**Corollary 2:** If a family  $f_c(x)$  is  $C^1$  with respect to  $x$  and a parameter  $c$  and has invariant probability density  $p_c$  depending continuously on  $c$  and  $x$  then  $\rho$  is differentiable with respect to  $c$  and

$$\frac{d\rho}{dc} = \int_0^\pi p_c(x) p_c(f(x)) \frac{\partial f}{\partial c}(x) dx.$$

**Proof:**

$$\rho(c') - \rho(c) = \int_A p_{c'}(x) p_c(x') dx' dx = \int p_{c'}(x) (f_{c'} - f_c)(x) p_c(x') dx$$

for some  $x'(x, c')$  between  $f_c(x)$  and  $f_{c'}(x)$ . The integrand is within  $o(c' - c)$  of  $\frac{\partial f}{\partial c}(x) p_c(f(x))(c' - c)$  and  $p_{c'}$  is within  $o(1)$  of  $p_c$ . Hence the result.

In particular, we apply this corollary to the time- $T$  map for (20). If the rotation rate for some value of  $c$  is not a multiple of  $\pi/T$  then the conditions of Corollary 2 are met and the integrand is negative everywhere, so  $\frac{d\rho}{dc} < 0$ .

### Appendix B.

Here the formula (28) for  $d\lambda_1/dc$  at  $c = 0$  is proved.

When the Floquet multipliers are real and positive, as near  $c = 0$ , the Lyapunov exponents are the real numbers  $\lambda$  such that there is a non-zero solution  $\zeta = e^{\lambda t}P(t)$  of the linearised equation  $\dot{\zeta} = L_c\zeta$  with  $P$  of period  $T$ . This can be regarded as an eigenvalue-eigenvector problem for  $(\lambda, P)$ :

$$L_c P - \dot{P} = \lambda P. \quad (33)$$

Since a linear operator and its adjoint have the same eigenvalues, there is a non-zero solution  $A = e^{-\lambda t}B(t)$  of the adjoint equation  $\dot{A} = -AL_c$  on linear functionals, with  $B$  of period  $T$ , i.e.

$$BL_c + \dot{B} = \lambda B. \quad (34)$$

For distinct Lyapunov exponents (as near  $c = 0$ ), the exponent and eigenvectors depend differentiably on  $c$ . So letting  $\pi = dP/dc$ ,  $L' = dL_c/dc$ ,  $\lambda' = d\lambda/dc$ , differentiating (33) with respect to  $c$  yields

$$\dot{\pi} + \lambda\pi - L_c\pi = L'P - \lambda'P \quad (35)$$

Apply the linear functional  $B(t)$  to (35) and integrate over one period in  $t$ :

$$\int_0^T B\dot{\pi} + \lambda B\pi - BL_c\pi \, dt = \int_0^T BL'P - B\lambda'P \, dt \quad (36)$$

Integrate the first term by parts and use (34) to see that the left hand side is zero. Now  $BP$  is constant (apply (33) and (34) to  $\frac{d(BP)}{dt} = \dot{B}P + B\dot{P}$ ) and non-zero, so by scaling  $B$  we can take  $BP = 1$ . Thus (36) yields

$$\lambda' = \frac{1}{T} \int_0^T BL'P \, dt \quad (37)$$

Now  $L' = \begin{bmatrix} 0 & 0 \\ -1 & 0 \end{bmatrix}$ , and at  $c = 0$  we can take  $\lambda = 0$ ,  $P(t) = (\dot{x}(t), \dot{y}(t))$ . So

$$\lambda'(0) = -\frac{1}{T} \int_0^T B_2(t)\dot{x}(t) \, dt, \quad (38)$$

as claimed.

### REFERENCES

- [1] S. Boccaletti, V. Latorab, Y. Moreno, M. Chavez, D. U. Hwang, Complex networks: Structure and dynamics, *Physics Reports* 424 (2006), 175-308.
- [2] L. M. Pecora and T. L. Carroll, Master Stability Functions for Synchronized Coupled Systems, *Phys. Rev. Lett.* 80(10) (1998), 2109-2112
- [3] T. Zhou, C. Guanrong, L. Qishao and X. Xiaohua, On estimates of Lyapunov exponents of synchronized coupled systems, *Chaos*, 16 (2006) 033123
- [4] D. Hansel and H. Sompolinsky, Synchronization and computation in a chaotic neural network, *Phys. Rev. Lett.* **68** (1992), 718–721 .
- [5] D. Hansel, Synchronized chaos in local cortical circuits, *Int. J. Neural Sys.* **6** (1996), 403-.
- [6] F. Pasemann, Synchronized chaos and other coherent states for two coupled neurons, *Physica D*, **128** (1999) 236-249 .
- [7] H. G. Winful and L. Rahman, Synchronized chaos and spatiotemporal chaos in arrays of coupled lasers, *Phys. Rev. Lett.* **65** (1990), 1575-
- [8] R. Li and T. Erneux, Bifurcation to standing and traveling waves in large arrays of coupled lasers, *Phys. Rev. A* **49** (1994), 1301–1312
- [9] R. Roy and K. S. Thornburg, Jr., Experimental synchronization of chaotic lasers, *Phys. Rev. Lett.* **72** (1994), 2009–2012

- [10] K. Otsuka, R. Kawai, S. Hwang, J. Ko and J. Chern, Synchronization of Mutually Coupled Self-Mixing Modulated Lasers, *Phys. Rev. Lett.* **84** (2000), 3049–3052
- [11] P. Wofo and H. G. Enjieu Kadji, Synchronized states in a ring of mutually coupled self-sustained electrical oscillators, *Phys. Rev. E* **69** (2004) 046206
- [12] S. Boccaletti, J. Kurths, G. Osipov, D. L. Valladares and C. S. Zhou, The synchronization of chaotic systems, *Physics Reports*, **366** (2002), 1-101
- [13] H. K. Leung, Critical slowing down in synchronizing nonlinear oscillators, *Physical Review E* **58** (1998), 5704–5709
- [14] P. Wofo, R.A. Kraenkel, Synchronization: Stability and duration time, *Physical Review E* **65** (2002), 036225
- [15] A. Pikovsky, M. Rosenblum and J. Kurths, *Synchronization, A Universal concept in Nonlinear Science*, Cambridge University Press (2001).
- [16] K. Fukui and S. Nogi, *IEEE Trans. Microwave Theory Tech.* Vol.MTT-28 (1980), 1059-
- [17] K. Fukui and S. Nogi, *IEEE Trans. Microwave Theory Tech.* Vol. MTT-34 (1986), 943-
- [18] A. Oksasoglou and D. Vavrim, *IEEE Trans. Circuits Syst.* **41** (1994), 6690-
- [19] J. F. Heagy, T. L. Carroll and L. M. Pecora, Synchronous chaos in coupled oscillator systems, *Phys. Rev. E* **50** (1994), 1874–1885
- [20] J. Guckenheimer and P. J. Holmes, *Nonlinear oscillations, dynamical systems and Bifurcations of vector fields* (Springer, 1983).
- [21] J. F. Heagy, L. M. Pecora and T. L. Carroll, Short Wavelength Bifurcations and Size Instabilities in Coupled Oscillator Systems, *Phys. Rev. Lett.* **74** (1995), 4185–4185
- [22] F. V. Atkinson, *Discrete and continuous boundary problems* (Academic, 1964).
- [23] VN Belykh, IV Belykh, M Hasler, Connection graph stability method for synchronised coupled chaotic systems, *Physica D* **195** (2004) 159–187.
- [24] K. S. Fink, G. Johnson, T. Carroll, D. Mar, and L. Pecora. Three coupled oscillators as a universal probe of synchronization stability in coupled oscillator arrays. *Phys. Rev. E*, **61**(5) (2000) 5080-5090
- [25] W. Lu and T. Chen. Synchronization of coupled connected neural networks with delays. *IEEE Trans. Circuit and Syst. I*, **51** (2004) 2491-2503  
W. Lu and T. Chen. New approach to synchronization analysis of linearly coupled ordinary differential systems. *Phys. D* **213** (2006) 214–230

Received July 2007; revised November 2007.

*E-mail address:* ryamapi@yahoo.fr (R.Yamapi)

*E-mail address:* R.S.MacKay@warwick.ac.uk (R. S. MacKay)